Cureus Journal of Engineering

Open Access Original Article

Bridging the Gap Between Theory and Computation: Sparse Polynomial Chaos Modeling of Uncertain Wood Properties in Musical Instrument Soundboards

Received 05/16/2025
Review began 05/18/2025
Review ended 08/06/2025
Published 08/09/2025

DOI:
https://doi.org/10.7759/s44388-025-06603-4

Akın Oktav [1] , Murat A. Başaran [2]

1. Department of Mechanical Engineering, Alanya Alaaddin Keykubat University, Antalya, TUR 2. Department of Industrial Engineering, Alanya Alaaddin Keykubat University, Antalya, TUR

Corresponding author: Akın Oktav, akin.oktav@alanya.edu.tr

Abstract

The rectangular plate with holes (RPwH) is a key component of many wooden string musical instruments, such as the guitar, fiddle, tamboura, and oud. One of the most important challenges in modeling wooden stringed musical instruments is the uncertainty arising from the mechanical properties of the materials. The sound produced by stringed instruments is designed by the vibrations of thin wooden shells and the soundboard (SB) is a critical component. In this study, the orthotropic mechanical properties of SBs are addressed, and their distributions are detected based on data sets and modeled to better account for uncertainty in statistical settings. The values of the flexural rigidities appeared in the well-known partial differential equation (PDE) for the calculation of the natural frequencies are assumed to be random variables with a distribution. The SB model is first approximated to a RPwH and then to a regular rectangular plate (RP). Deviations between the analytical solution and simulation results are based on the random variables. A polynomial chaos expansion (PCE) is constructed for the solution. Although there is no closed-form solution for the SB with holes, the so-called sparse PCE with a copula structure between these three geometries is obtained with a very small error value. The first 100 natural frequencies were computed for the RP, the RPwH, and the SB, with deviations observed between simulation and PDE solution results. The mean value of the PCE model was found to be 700 with a standard deviation of 1,349 and a coefficient of variation of 171.5%. The proposed analytical modeling framework can be used for uncertainty quantification and validation in any study of orthotropic RPs.

Categories: Structural Analysis and Finite Element Analysis, Structural Engineering, Data Science and Analytics for Engineering
Keywords: uncertainty quantification, soundboard, polynomial chaos expansion, orthotropic material, structural analysis

Introduction

Literature on musical instruments has improved significantly over the past decades. Addressing the topic through an engineering perspective, computational modeling and acoustic analysis of musical instruments are of great importance in terms of standardization and sustainability [1,2].

Instrument makers and players are negatively affected by uncertainty. It is important for engineers and researchers to work on this issue and provide support. Another important issue is environmental concerns: some tree species may become extinct or their use may be restricted in the near future. The first step in developing alternative engineering materials is to make reliable models of existing wooden musical instruments.

Modeling of musical instruments essentially is performed to predict the vibration and acoustics characteristics of the instrument [3]. A common approach is to conduct a modal analysis study using a verified model [4]. To construct a verified computational model of the wooden stringed musical instruments, deterministic element-based methods such as finite element method and boundary element method are used [5,6]. Since these instruments are resonance boxes containing acoustic cavities, a vibroacoustic modeling is also required which considers a weak (one-way) fluid structure coupling [7,8]. Experimental modal analysis results are used to verify and refine the computational model [9].

In the approach outlined above, the challenge is mostly due to uncertainties arising from manufacturing procedures and material properties [10,11]. Since wood is a natural orthotropic material, even if the geometry is known exactly from 3D scanning or other reverse engineering tools, the mechanical properties of the materials are not exactly known. It is possible to measure these properties, but they are still exact only for the measured samples. Since the internal structure of the material is not homogeneous, the measured properties exhibit a spatial distribution [12-15].

In terms of manufacturing, the professional musical instruments are often made by the experienced luthiers who strictly follow the design constraints determined from the past experiences. Due to uncertainties, the sound produced by the instrument may require a fine tuning after production. The tools for the fine tuning are very limited and one of them is to change or modify the soundboard (SB). The sound produced by the stringed instruments are designed by the vibrations of thin wooden shells and the SB is a critical component. It also affects the fluid-structure interaction, and it has sound holes which radiates the sound from the cavity in terms of Helmholtz resonance. The number and shape of sound holes varies. The classical guitar has one oval sound hole [5], the violin has two *f*-holes [15], and the oud has three sound holes of different sizes [16].

In the current work, the orthotropic mechanical properties of SBs are addressed. For thin wooden plates, nine material properties are required for a computational model, and three of them, the flexural rigidities (D_x, D_y, D_{xy}), are assumed to be random variables having probability distributions. A polynomial chaos expansion (PCE) model [17-19] is constructed based on the random D_x, D_y, D_{xy} variables and the residuals, which are the random input variables in the model. Calculations are performed on an oud SB as a case study.

Materials And Methods

Calculation of natural frequencies

The motivation for the research problem is two-fold. While the first phase is related to constructing a sparse PCE that models simulation data more accurately than does the solution of the partial differential equation (PDE) for an orthotropic rectangular plate (RP), which was solved in [20], the second phase is to employ this modeling approach to search for the solution of another geometric structure called SB, whose closed-form mathematical function is not available in the literature. Assuming simple harmonic motion, the PDE for the transverse bending of a plate having rectangular orthotropy is

$$D_x \frac{\partial^4 w}{\partial x^4} + 2D_{xy} \frac{\partial^4 w}{\partial x^2 \partial y^2} + D_y \frac{\partial^4 w}{\partial y^4} - \rho \omega^2 w = 0$$

where ω is the natural frequency; w is the displacement in the z-direction; a and b are the length and the width of the plate; D_x, D_y, D_{xy} are the flexural rigidities; ρ is the density; m and n are integers. Equation (1) is solved to determine the first 100 natural frequency (ω) values, where all the results are tabulated in the Appendix. However, when simulation data and the solution of the PDE for a Sitka spruce RP with the dimensions 490 mm × 396 mm × 2 mm are compared graphically for the first 100 natural frequencies, deviations are observed as shown in Figure *1*, called residuals, between those outcomes. Note that, as the frequency value is increased, the deviation between the simulation results and the outcomes of the solution method tends to increase except for a few observations. The accuracy of the approximate solution decreases in higher modes. It suggests that a more refined mathematical expression is required, which indicates that the solution procedure proposed in [20] is an approximate solution. It is known that the approximate solution of Equation (1) is obtained using the Rayleigh-Ritz method by Hearmon [21].

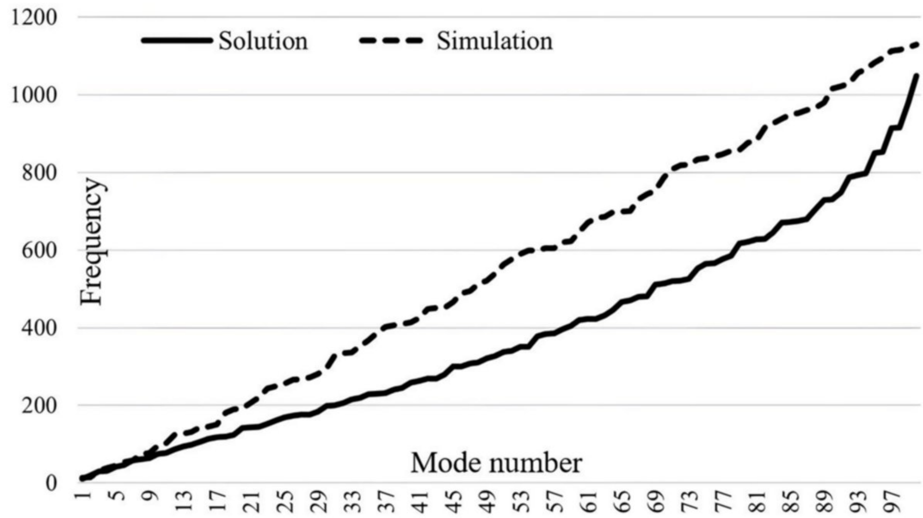

FIGURE 1: Comparison between the simulation and the PDE solution results for the first 100 mode values

Frequency vs mode number. PDE, partial differential equation

Simplified analytical models of the soundboard

The oud's SB can be modeled as a RP, which can be further simplified to a rectangular plate with holes (RPwH) to derive an analytical solution. The mechanical properties of the SB material, Sitka spruce, are tabulated in Table *1* [22]. The FE model is created using 10-noded 3D elements having a maximum size of 5 mm, and the number of elements are 41,753.

Wood	Density	Young's moduli (MPa)			Shear moduli (MPa)			Poisson's ratios					
	kg/m^3	E_L	E_T	E_R	G_{LT}	G_{LR}	G_{RT}	V_{LT}	V_{LR}	V_{RT}	V_{TL}	V_{RL}	V_{TR}
Spruce, Sitka	360	9,900	772	426	634	604	30	0.372	0.467	0.435	0.040	0.025	0.245

TABLE 1: Mechanical properties of Sitka spruce with 12% moisture content. (L (longitudinal): x-direction, T (transverse): y-direction, R (radial): z-direction.)

In what follows, the simplified analytical models of the SB are derived from its computational model. The shapes, dimensions, and the first 10 natural frequency values of the models are tabulated in Table *2*. The proposed analytical solution is explained and implemented through simplified models. Through a statistical assessment, high correlations in the same direction are observed between the mode frequency values of the pairwise geometries i.e., the RP, the RPwH, and the SB (see Figure *2*).

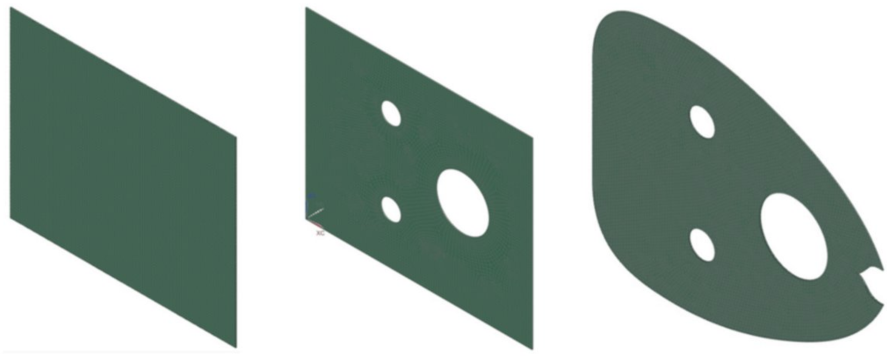

FIGURE 2: Rectangular plate, rectangular plate with holes and soundboard

Geometry	Rectangular plate	Rectangular plate with holes	Soundboard
Dimensions (*l, w, h*) in mm	490, 396, 2	490, 396, 2	490, 396, 2
1st natural freq.	13.82 Hz	13.13 Hz	16.41 Hz
2nd natural freq.	14.26 Hz	13.78 Hz	18.99 Hz
3rd natural freq.	31.49 Hz	31.26 Hz	39.15 Hz
4th natural freq.	39.27 Hz	39.06 Hz	43.32 Hz
5th natural freq.	45.03 Hz	39.76 Hz	52.76 Hz
6th natural freq.	52.89 Hz	50.92 Hz	63.57 Hz
7th natural freq.	57.43 Hz	56.69 Hz	79.00 Hz
8th natural freq.	73.03 Hz	68.69 Hz	91.11 Hz
9th natural freq.	77.34 Hz	78.34 Hz	97.69 Hz
10th natural freq.	94.57 Hz	94.54 Hz	120.73 Hz

TABLE 2: First 10 natural frequency values of the soundboard and the simplified geometries computed under free boundary conditions

Results

Briefly, even though the conventionally resolved problems provide an idealized solution, their solutions are reached under ideal conditions. When the ideal conditions are subject to alterations such as randomness, interval representation, or a combination of them, the supposedly ideal solutions are no longer valid. Thus, PCE has been widely substituted with deterministically solved problems responding to those alterations by introducing the randomization of input parameters [23]. Deviations, namely residuals, can be computed by

$$Res_i = MSol_i - MSim_i; i = 1, 2, ..., 100$$

where *MSol* and *MSim* represent the outcomes of the solution of the PDE and the outcomes of the experimental or simulation conduct, respectively. Residuals vary in an interval between -296.27 and 4.98

for the orthotropic RP (see Appendix). To find a more representative mathematical model for non-intrusive investigation and predictive purposes, the parameters existing in Equation (1) are assumed to be D_x, D_y, and D_z. In other words, uncertainty related to those parameters is the core source of deviations between simulation and PDE solution results. For this purpose, PCE is constructed based on random D_x, D_y, and D_z variables and the residuals, which are the random input variables in the model. To determine the probability distributions of the random variables, and residuals, a kernel density estimate for each is obtained by utilizing R Studio v4.3 3. Figure 3 depicts the inferred distribution for the residuals. Therefore, a PCE model is obtained using Matlab v.24.1 and UQLab v2.0 on a laptop with an i5 processor [24]. The outcomes of the model are tabulated in Table 3, and Figure 4 and Figure 5 display distributions of the input variables and the fitting of the proposed model. Figure 4 depicts two distinct graph types. The diagonal graphs present the probability distributions of the stochastic variables. The off-diagonal graphs depict the associated graphs between different stochastic attributes.

Model information	Results
Number of input variables	4
Maximal degree	1
q-norm	0.5
Size of full basis	5
Size of sparse basis	3
Full model evaluations	100
Leave-one-out error	9.3e-3
Modified leave-one-out error	1.2e-3
Mean value	700.04
Standard deviation	884.92
Coefficient of variation	126.4 (Percent)

TABLE 3: The outcomes of the PCE model

PCE, polynomial chaos expansion

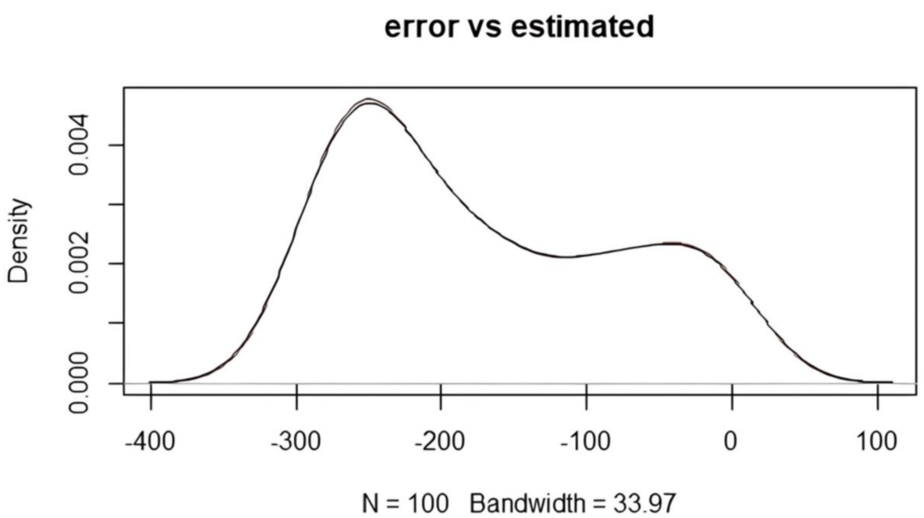

FIGURE 3: Kernel estimates of residuals

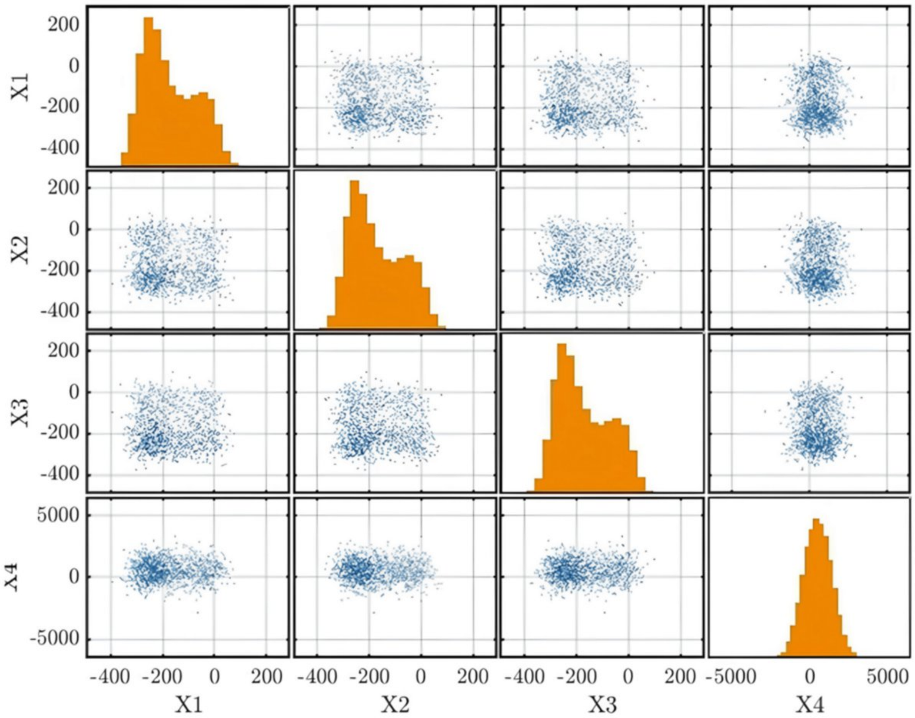

FIGURE 4: The graphs of four input variables used in PCE, where the random input variables X1, X2, X3, X4 correspond to Dx, Dy, Dxy, and the residuals, respectively

In the scatter plot matrix, each cell represents a scatter plot of one variable against another. PCE, polynomial chaos expansion

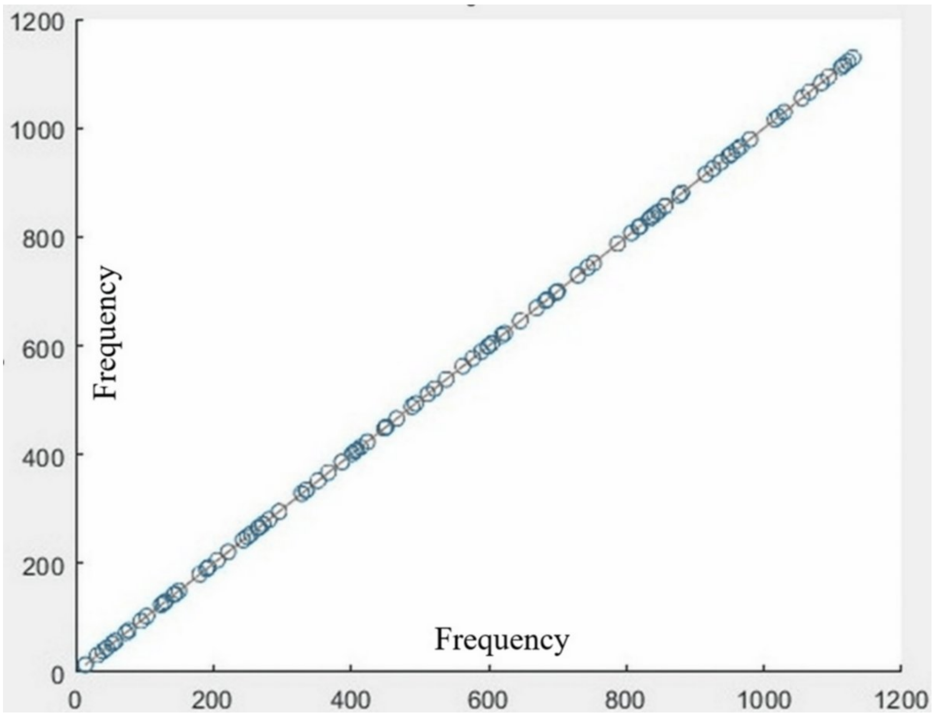

FIGURE 5: The graph of the model fitting

The PCE model constructed for the orthotropic RP is expanded into the RPwH and then into the actual SB of the oud. Even though a closed-form solution is available for an orthotropic RP represented by a PDE, it is not true for both the RPwH and the SB. For this purpose, correlation coefficients are first computed between those geometries to understand how those geometries are related statistically where the results are tabulated in Table 4.

Geometries	Rectangular plate	Rectangular plate with holes	Soundboard
Rectangular plate	1.00	1.00	0.99
Rectangular plate with holes	Symmetry	1.00	0.99
Soundboard	Symmetry	Symmetry	1.00

TABLE 4: The correlation coefficients of the three geometries

All correlations are computed by SPSS 27.0 version and tested at a 0.05 significance level. All correlation coefficients are found to be statistically significant. The results suggest that the three geometries are highly correlated. However, further analysis is required to construct a PCE model for SB; so, new variables representing ratios of two different geometries are generated and correlations between them are computed to determine how they are related. The results are tabulated in Table 5.

Geometries	RP/SB	RP/RPwH	RPwH/SB
RP/SB	1.00	0.448	0.789
RP/RPwH	Symmetry	1.00	-0.196
RPwH/SB	Symmetry	Symmetry	1.00

TABLE 5: The correlations between inputs of geometries

RP, rectangular plate; RPwH, rectangular plate with holes; SB, soundboard

Table 5 suggests that to determine the PCE model for SB, copula needs to be defined between the inputs of geometries. To verify further, factor analysis is run to determine how those solutions are grouped statistically. All solutions are statistically inseparable, which means that all solutions are statistically related. The results of RP, RPwH, SB, and PDE are tabulated in Table 6.

Numerical results	Factor 1	Factor 2
RP	0.721	0.693
RPwH	0.734	0.678
SB	0.715	0.699
Solution of PDE	0.671	0.720

TABLE 6: Rotated factor scores

RP, rectangular plate; RPwH, rectangular plate with holes; SB, soundboard

Table 6 suggests that all geometrical shapes are highly statistically related. Thus, the implemented PCE utilizes a copula structure to represent the correlated input variables. The results of the PCE model for SB are tabulated in Table 7.

Model information	Results
Number of input variables	4
Maximal degree	1
q-norm	0.50
Size of full basis	5
Size of sparse basis	3
Full model evaluations	100
Leave-one-out error	9.3e-3
Modified leave-one-out error	1.6e-3
Mean value	700.0413
Standard deviation	1,348.6805
Coefficient of variation	171.531 (Percent)

TABLE 7: The outcomes of the PCE model of the soundboard

PCE, polynomial chaos expansion

The results tabulated in Table *5* imply that four correlated random input variables need to be represented as a copula in the constructed PCE model to estimate modal characteristics of SB. The constructed model has a superior fit between the simulation results and the PDE solution results with a 9.3e-3 leave-one out error score.

Discussion

To construct a reliable computational model of the SB, an analytical verification study is conducted. As the relevant literature suggests, one of the most important components of the stringed musical instruments is the SB in terms of acoustic characteristics. Hence, an analytical verification study is performed on the SB through its simplified models, namely a RP and a RPwH, where all dimensions are compatible with those of the actual SB.

The solution method of RP that is solidly based on the PDE proposed by [20,21] is studied. However, when the simulation results and solutions of the proposed mathematical model are compared, residuals are observed concerning all mode frequency values. Therefore, it is assumed that the differences stem from the assumption of fixed parameters (D_x, D_y, D_{xy}), which are certainly not constant in any natural orthotropic material. This part of the research concludes that a better representable mathematical model including the uncertainty stemming from those parameters is needed.

A sparse PCE is utilized to construct a sparse polynomial model accounting for simulation data concerning the three random input variables, which are the parameters that are assumed to be fixed, and the last input parameter, which is the residuals of the mathematical model. Therefore, four input variables whose probability distributions are inferred as kernel density distributions are determined. Consequently, the sparse PCE model that generates a model with leave-one-out error criterion 9.3e-3 is derived.

Since the three geometries introduced in Table *2* are highly correlated, the derivation of a sparse PCE concerning the SB is closely related to the analytical solution of the RP in a statistical way, that is represented by statistical analysis, called correlation. Those correlations are represented via a copula structure. Therefore, the mathematical representation of the SB, expressed by PCE, is achieved.

Conclusions

In this research, sparse PCE is utilized within a probabilistic framework to construct an analytical verification model for the SB. Instead of employing deterministic variables to express the relationship between input and output variables for the mathematical model, random input variables with predefined probability distributions that are orthogonal to the family of multivariate polynomials are utilized to represent the relationship. The steps are as follows:

The first 100 natural frequencies were computed for the RP, the RPwH, and the SB. Deviations were observed between simulation and PDE solution results, with residuals varying between -296.27 and 4.98.

The mean value of the PCE model was found to be 700 with a standard deviation of 1,349 and a coefficient of variation of 171.5%.

The constructed model has a superior fit between the simulation results and the PDE solution results with a 9.3e-3 leave-one-out error score.

Even though there exists no closed-form solution for the SB, the model called sparse PCE with copula structure between these three geometries is attained with a very infinitesimal error value. The proposed analytical modeling framework can be used for uncertainty quantification and verification purposes in any study concerning the orthotropic RPs.

Appendices

The first 100 natural frequencies are computed for the RP, the RPwH, and the SB. The natural frequencies of the RP are also calculated by solving the PDE (Equation 1). The error between the computational and analytical results is calculated. The results are tabulated in Table 8 for comparison.

Mode #	Rectangular plate	Rectangular plate with holes	Soundboard	The solutions of PDE for the rectangular plate	Error (calculation-computation)
1	13.82	13.13	16.41	10.49	-3.33
2	14.26	13.78	18.99	19.24	4.98
3	31.49	31.26	39.15	29.91	-1.58
4	39.27	39.06	43.32	31.00	-8.27
5	45.03	39.76	52.76	41.95	-3.08
6	52.89	50.92	63.57	46.02	-6.87
7	57.43	56.69	79.00	57.95	0.52
8	73.03	68.69	91.11	61.30	-11.73
9	77.34	78.34	97.69	64.57	-12.77
10	94.57	94.54	120.73	75.03	-19.54
11	103.21	99.98	137.56	76.97	-26.24
12	124.17	117.52	142.15	86.83	-37.34
13	127.38	127.03	143.27	94.38	-33.00
14	130.49	128.57	167.00	98.94	-31.55
15	142.76	137.08	179.78	105.03	-37.73
16	144.29	143.54	198.54	112.90	-31.39
17	149.86	150.47	200.70	117.58	-32.28
18	180.38	176.63	217.73	119.64	-60.74
19	189.97	189.05	220.81	124.00	-65.97
20	192.86	192.16	245.44	141.22	-51.64
21	206.05	201.28	269.00	142.83	-63.22
22	221.38	205.88	273.60	143.92	-77.46
23	243.15	231.01	289.71	152.32	-90.83
24	248.91	244.22	292.93	161.18	-87.73
25	254.38	248.48	307.18	167.78	-86.60
26	265.01	258.64	339.35	173.19	-91.82

27	266.80	266.13	346.07	176.29	-90.51
28	272.25	273.88	361.02	176.66	-95.59
29	280.81	283.09	361.84	184.06	-96.75
30	295.49	285.85	379.80	198.17	-97.32
31	328.25	315.12	410.78	199.32	-128.93
32	334.46	327.74	422.22	205.39	-129.07
33	335.51	338.25	425.28	214.41	-121.10
34	352.17	354.67	441.96	219.35	-132.82
35	367.20	367.05	450.12	228.40	-138.80
36	386.49	371.67	457.55	229.79	-156.70
37	401.80	391.94	500.10	231.78	-170.02
38	405.99	402.51	500.64	240.63	-165.36
39	408.74	411.17	508.84	245.19	-163.55
40	413.88	413.80	538.11	258.27	-155.61
41	423.44	420.88	539.74	262.16	-161.28
42	448.27	435.81	552.52	268.38	-179.89
43	450.59	443.91	564.09	269.19	-181.40
44	451.30	458.50	597.87	279.01	-172.29
45	466.29	468.87	616.76	299.72	-166.57
46	488.15	482.24	618.71	300.13	-188.02
47	493.58	501.67	647.33	307.89	-185.69
48	511.45	502.71	653.56	310.86	-200.59
49	521.18	515.49	664.29	320.65	-200.53
50	538.28	535.26	700.42	326.45	-211.83
51	562.36	568.23	703.30	336.58	-225.78
52	576.76	575.81	710.98	340.58	-236.18
53	589.41	583.13	720.59	350.33	-239.08
54	598.70	588.03	735.16	351.11	-247.59
55	599.40	597.26	743.55	377.51	-221.89
56	604.50	605.38	764.21	383.41	-221.09
57	604.66	606.22	788.82	384.49	-220.17
58	618.89	625.77	809.68	395.77	-223.12
59	622.95	637.69	829.18	404.40	-218.55
60	645.76	639.77	834.91	420.11	-225.65
61	669.84	661.76	848.18	421.99	-247.85
62	682.40	688.48	858.51	422.24	-260.16
63	685.30	701.05	862.47	431.33	-253.97
64	697.78	704.83	911.97	445.24	-252.54
65	699.42	710.83	917.64	465.73	-233.69
66	700.03	727.36	937.63	470.32	-229.71

67	729.51	739.34	950.84	478.56	-250.95
68	743.59	753.90	958.26	481.08	-262.51
69	752.29	766.99	981.91	510.40	-241.89
70	787.43	798.01	983.81	513.84	-273.59
71	807.21	801.92	992.08	518.80	-288.41
72	817.78	823.59	1,023.00	521.51	-296.27
73	819.84	825.25	1,046.00	526.20	-293.64
74	832.84	827.84	1,054.00	551.68	-281.16
75	836.90	836.80	1,081.00	564.87	-272.03
76	840.85	840.36	1,091.00	565.72	-275.13
77	846.19	842.11	1,096.00	575.68	-270.51
78	855.90	866.14	1,115.00	585.76	-270.14
79	856.79	870.29	1,115.00	615.87	-240.92
80	876.56	876.54	1,144.00	621.02	-255.54
81	880.52	886.32	1,183.00	627.32	-253.20
82	915.15	928.15	1,197.00	628.87	-286.28
83	925.42	934.57	1,205.00	644.74	-280.68
84	936.99	950.96	1,211.00	670.47	-266.52
85	948.37	973.09	1,215.00	671.13	-277.24
86	952.30	980.58	1,239.00	675.28	-277.02
87	960.33	983.45	1,242.00	679.47	-280.86
88	965.60	988.56	1,264.00	705.15	-260.45
89	979.25	998.99	1,276.00	728.75	-250.50
90	1,016.00	1,025.00	1,296.00	730.18	-285.82
91	1,021.00	1,047.00	1,306.00	747.75	-273.25
92	1,029.00	1,064.00	1,329.00	786.97	-242.03
93	1,055.00	1,070.00	1,332.00	792.67	-262.33
94	1,066.00	1,102.00	1,338.00	797.27	-268.73
95	1,083.00	1,104.00	1,345.00	849.40	-233.60
96	1,094.00	1,112.00	1,364.00	852.82	-241.18
97	1,112.00	1,119.00	1,381.00	913.62	-198.38
98	1,116.00	1,125.00	1,416.00	915.61	-200.39
99	1,122.00	1,134.00	1,419.00	979.06	-142.94
100	1,129.00	1,135.00	1,426.00	1,048.65	-80.35

TABLE 8: Comparison of the results

Additional Information

Author Contributions

All authors have reviewed the final version to be published and agreed to be accountable for all aspects of the work.

Concept and design: Akın Oktav

Acquisition, analysis, or interpretation of data: Akın Oktav, Murat A. Başaran

Drafting of the manuscript: Akın Oktav

Critical review of the manuscript for important intellectual content: Akın Oktav, Murat A. Başaran

Supervision: Akın Oktav

Disclosures

Human subjects: All authors have confirmed that this study did not involve human participants or tissue. **Animal subjects:** All authors have confirmed that this study did not involve animal subjects or tissue. **Conflicts of interest:** In compliance with the ICMJE uniform disclosure form, all authors declare the following: **Payment/services info:** All authors have declared that no financial support was received from any organization for the submitted work. **Financial relationships:** All authors have declared that they have no financial relationships at present or within the previous three years with any organizations that might have an interest in the submitted work. **Other relationships:** All authors have declared that there are no other relationships or activities that could appear to have influenced the submitted work.

References

1. Dunn F, Hartmann WM, Campbell DM, Fletcher NH: Springer Handbook of Acoustics. Springer Verlag, New York; 2015. 10.1007/978-1-4939-0755-7
2. Chaigne A, Kergomard J: Acoustics of Musical Instruments. Springer, New York; 2016. 10.1007/978-1-4939-3679-3
3. Atre MP, Apte SD: Generalized modeling of body response of acoustic guitar for all frets using a response for single fret. Applied Acoustics. 2019, 145:439-44. 10.1016/j.apacoust.2018.10.017
4. Curtu I, Stanciu M, Baba MA: The numerical modeling of the acoustic plates on the guitar structures. Annuals of the University of Petrosani-Mechanical Engineering. 2008. 10:41-46.
5. Gorrostieta-Hurtado E, Pedraza-Ortega JC, Ramos-Arreguin JM, Sotomayor-Olmedo A, Perez-Meneses J: Vibration analysis in the design and construction of an acoustic guitar. International Journal of the Physical Sciences. 2012, 7:1986-97.
6. Kaselouris E, Bakarezos M, Tatarakis M, Papadogiannis NA, Dimitriou V: A review of finite element studies in string musical instruments. Acoustics. 2022, 4:183-202.
7. Ribeiro R, Inácio O: Experimental modal analysis of a fully assembled Portuguese guitar. Actas del congreso EuroRegio. Oporto, Portugal; 2016. 1-10.
8. Vieira M, Infante V, Serrão P, Ribeiro AMR: Experimental-numerical correlation of the dynamic behavior of the Portuguese guitar. Applied Acoustics. 2018, 131:51-60. 10.1016/j.apacoust.2017.10.007
9. Patil K, Baqersad J, Ludwigsen D, Dong Y: Extracting vibration characteristics of a guitar using finite element, modal analysis, and digital image correlation techniques. Proceedings of Meetings on Acoustics, Acoustical Society of America. 2016, 29:065003. 10.1121/2.0000465
10. Torres JA, de Icaza-Herrera M, Castaño VM: Guitar acoustics quality: Shift by humidity variations. Acta Acustica united with Acustica. 2014, 100:537-42. 10.3813/aaa.918733
11. Ahmed SA, Adamopoulos S: Acoustic properties of modified wood under different humid conditions and their relevance for musical instruments. Applied Acoustics. 2018, 140:92-99. 10.1016/j.apacoust.2018.05.017
12. Wegst UGK: Wood for sound. American Journal of Botany. 2006, 93:1439-448. 10.3732/ajb.93.10.1439
13. Dumond P, Baddour N: Experimental investigation of the mechanical properties and natural frequencies of simply supported Sitka spruce plates. Wood Science and Technology. 2015, 49:1137-155. 10.1007/s00226-015-0759-z
14. Krüger R, Buchelt B, Wagenführ A: New method for determination of shear properties of wood. Wood Science Technology. 2018, 52:1555-568. 10.1007/s00226-018-1053-7
15. Stanciu MD, Coşereanu C, Dinulică F, Bucur V: Effect of wood species on vibration modes of violins plates. European Journal of Wood and Wood Products. 2020, 78:785-99. 10.1007/s00107-020-01538-5
16. İnanlı S, Altınsoy E: Vibroacoustics of Oud. DAGA 2018. German Acoustical Society, München; 2018. 923-25.
17. Wei Y, Vazeille F, Serra Q, Florentin E: Hybrid Polynomial Chaos Expansion and proper generalized decomposition approach for uncertainty quantification problems in the frame of elasticity. Finite Elements in Analysis and Design. 2022, 212:103838. 10.1016/j.finel.2022.103838
18. Sudret B, der Kiureghian A: Stochastic finite element methods, and reliability: a state-of-the-art report. Report No. UCB/SEMM-2000/08. Department of Civil and Environmental Engineering, University of California. Report No. UCB/SEMM-2000/08, Berkeley; 2000.
19. Blatman G, Sudret B: Adaptive sparse polynomial chaos expansion based on least angle regression. Journal of Computational Physics. 2011, 230:2345-367. 10.1016/j.jcp.2010.12.021
20. Leissa AW: Vibration of Plates. Scientific and Technical Information Division, National Aeronautics and Space Administration, 1969.
21. Hearmon RFS: The fundamental frequency of vibration of rectangular wood and plywood plates. Proceedings of the Physical Society. 1946, 58:1926-948. 10.1088/0959-5309/58/1/307
22. Kretschmann DE: Mechanical properties of wood. Wood Handbook: Wood as an Engineering Material. Ross RJ (ed): U.S. Department of Agriculture, Forest Service, Forest Products Laboratory, Madison, WI; 2010. 5-1/5-46.
23. Al-Bittar T, Soubra AH: Efficient sparse polynomial chaos expansion methodology for the probabilistic analysis of computationally-expensive deterministic models. International Journal for Numerical and Analytical Methods in Geomechanics. 2014, 38:1211-230. 10.1002/nag.2251

24. Marelli S, Bruno S: UQLab: A Framework for uncertainty quantification in Matlab. Vulnerability, Uncertainty, and Risk Proceedings, University of Liverpool, UK. 2014, 2554-563.